Title
Combining quantitative phase microscopy and laser-induced shockwave for the study of cell injury.

Journal
Biomedical Optics Express, 12(7)

ISSN
2156-7085

Authors
Pouladian, Pegah
Yamauchi, Toyohiko
Wakida, Nicole M
et al.

Publication Date
2021-07-01

DOI
10.1364/boe.427693

Peer reviewed

Research Article | Vol. 12, No. 7 / 1 July 2021 / Biomedical Optics Express 4020
Biomedical Optics EXPRESS

Combining quantitative phase microscopy and laser-induced shockwave for the study of cell injury

PEGAH POULADIAN,[1,4] TOYOHIKO YAMAUCHI,[2] NICOLE M. WAKIDA,[1] VERONICA GOMEZ-GODINEZ,[3] MICHAEL W. BERNS,[1] AND DARYL PREECE[1,5]

[1]*Beckman Laser Institute, Department of Biomedical Engineering, University of California Irvine, CA 92617, USA*
[2]*Hamamatsu Photonics K. K., 5000 Hirakuchi, Hamakita, Shizuoka 434-8601, Japan*
[3]*Institute of Engineering in Medicine, University of California, San Diego, San Diego CA 92093, USA*
[4]*ppouladi@uci.edu*
[5]*dpreece@uci.edu*

Abstract: In this paper, we propose a new system for studying cellular injury. The system is a biophotonic work station that can generate Laser-Induced Shockwave (LIS) in the cell culture medium combined with a Quantitative Phase Microscope (QPM), enabling the real-time measurement of intracellular dynamics and quantitative changes in cellular thickness during the damage and recovery processes. In addition, the system is capable of Phase Contrast (PhC) and Differential Interference Contrast (DIC) microscopy. Our studies showed that QPM allows us to discern changes that otherwise would be unnoticeable or difficult to detect using phase or DIC imaging. As one application, this system enables the study of traumatic brain injury in vitro. Astrocytes are the most numerous cells in the central nervous system (CNS) and have been shown to play a role in the repair of damaged neuronal tissue. In this study, we use LIS to create a precise mechanical force in the culture medium at a controlled distance from astrocytes and measure the quantitative changes, in order of nanometers, in cell thickness. Experiments were performed in different cell culture media in order to evaluate the reproducibility of the experimental method.

1. Introduction

Single-cell manipulation is increasingly utilized in biological research for analysis of cell characteristics such as the cell adhesion, interactions between cells, and intracellular movement of individual organelles such as chromosomes during cell division [1–4]. Biophotonic tools such as laser tweezers and/or scissors utilizing focused lasers to manipulate single cells are key developments for future studies in cell biology [5,6]. In this burgeoning field, LIS and its mechanical impact on cells is an area of significant interest [7].

Hosokawa et al. used a femtosecond laser to generate LIS in the medium containing mouse NIH3T3 fibroblasts cultured on a collagen matrix. The study has shown that using LIS, cells can be detached without any injuries, leading to a promising way to fine manipulation of the cells [5]. An Nd:YAG laser-driven flyer-plate technique has been used to generate LIS on endothelial cells as a reproducible method to study cellular membrane injuries and cell detachment from a surface [8].

LIS has been also shown to increase the plasma membrane and stratum corneum permeability in cells. This is a promising method to introduce various chemicals into cells non-invasively and may be of use for drug delivery and potentially for gene transfection [9,10].

With respect to the studies reported here, LIS has been shown to be an effective way to model traumatic brain injury (TBI) in vivo and in vitro [11]. For instance, LIS has been applied on

#427693 https://doi.org/10.1364/BOE.427693
Journal © 2021 Received 15 Apr 2021; revised 22 May 2021; accepted 24 May 2021; published 11 Jun 2021

Biomedical Optics EXPRESS

the skin surface of the left parietal region of the mouse brain, in vivo. The brain tissue has then been excised for further analysis. It was not possible to study the cellular changes during and immediately after the injury with this model [12].

LIS has been used to subject brain cells, in vitro, to a similar condition that cells experience during blast-induced traumatic brain injury by applying exact and controllable shear stress to the cells [13,14]. The response of hippocampal brain cells to injuries caused by LIS and sub-axotomy have demonstrated similar responses in terms of cytoskeletal dynamics. Although a wavelet algorithm has been used to quantitatively measure the induced damage to the cells, precise direct quantitative measurement of LIS damage has not been possible [15]. The study we report here addresses that methodological deficiency.

When an injury occurs to the brain, neuronal cells interact with each other to maintain the brain's normal function. Astrocytes, the most numerous cells in the CNS, play a crucial role in maintaining equilibrium between ions and maintaining homeostasis of water and the blood flow needed to maintain healthy tissue [16,17].

In the 1930s, Zernike created a technique, calling it phase contrast imaging, for imaging phase objects with high contrast without the requirement for labeling, which revolutionized intrinsic contrast imaging [18]. The phase contrast microscope is now is widely employed to observe living, unlabeled cells and other transparent objects in great detail [19]. Scientists can extract useful information from phase changes of light as it interacts with cells. Previous studies have used a variety of different techniques to acquire phase images of cells in order to extract valuable information about them [20]. For instance, one study has used digital holographic microscopy (DHM) to quantitatively measure cellular morphology, and proved that the early detection of neuron cell death is possible using quantitative phase images [21]. Another study has also used DHM and has shown that quantitative phase measurements of cells can be used to fully characterize cellular behaviour, like cellular height and volume, during exposure to pollutant metals like cadmium [22]. Cell volume changes under blue light exposure were also measured in another study. In this study, the blue laser light was used as a tool for holographic microscopy and also for inducing toxic effects on cells [23].

Quantitative phase imaging (QPI) is an emerging label-free method to study transparent cells and tissues without photo-bleaching effects often encountered with conventional fluorescence imaging. This modality uses interferometry to precisely quantify the phase shifts caused by the sample. This allows for imaging and quantification transparent features in cells, measuring movements of organelles, and quantification of cellular dynamics including membrane motility [19,24,–26]. In this study, we introduce a QPI system which enables quantitative phase imaging of cells before, during and after LIS exposure. We capture 3D images of LIS injury and quantitatively measure membrane changes, as well as internal cell structure in two types of cells.

2. Method

2.1. Theory

2.1.1. Laser-Induced Shockwave (LIS)

If a fluid is irradiated by pulsed laser light with an irradiance beyond its optical breakdown threshold, nonlinear absorption leads to photo-ionization and plasma formation. The difference in pressure and temperature of the plasma and the fluid causes the plasma to expand creating a cavitation bubble. The bubble expansion causes a shockwave, propagating several hundred microns within the fluid. This phenomenon can be used to damage cells by the mechanical force of the shockwave [15,27]. The bubble's expansion and contraction can put significant pressure on adjacent structures, particularly cells and the size of the bubble can be changed by the laser irradiance at the focus point [28,29]. The pressure gradient as a function of the distance from the

Biomedical Optics EXPRESS

center of the shockwave has been measured allowing for the calculation of the exact pressure the cells are exposed to [27,30].

2.1.2. Quantitative Phase Microscopy

Imaging of living cells is limited without using labeling techniques since they do not naturally absorb or scatter much light. However, we can extract valuable information from the phase changes of light as it interacts with the cells [20].

QPM is a new promising approach to study cell morphology including surface fluctuations of cells with nanometer resolution. In this system, light with the center wavelength of λ_c passes through a Linnik interferometer which divides it into two beams: one beam passes through the sample, while the other one is used as the reference beam. Both are reflected onto a CCD camera for interferogram acquisitions. The system used in this study uses a quarter-wavelength phase-shifting algorithm to calculate the phase-contrast images. The optical path-length is periodically shifted by $\lambda_c/4$ resulting in 4 interference images. The phase (θ) is calculated by the intensity $I_{(\theta)}$ of these 4 consecutive images based on Eq. (1) [30]:

$$\theta = \tan^{-1}\left(\frac{I_{(\frac{3\pi}{2})} - I_{(\frac{\pi}{2})}}{I_{(0)} - I_{(\pi)}}\right) \tag{1}$$

Based on the phase, the optical height (OH) is measured as follows in Eq. (2) [31]:

$$OH = \frac{\lambda_c}{2\pi} \times \frac{\theta}{2} \tag{2}$$

The real height (RH) of the cells is related to the optical height (OH) with the estimation of mean refractive index of the cells ($\bar{n}_{cell} \approx 1.37$) [31] and the medium ($n_{medium} \approx 1.337$) [32] based on the Eq. (3) [31]:

$$RH = \frac{OH}{\bar{n}_{cell} - n_{medium}} \tag{3}$$

A more detailed description on the QPM setup and the phase unwrapping process can be found in [31,33].

2.2. Setup

Our system is comprised of a laser that is introduced into a quantitative phase microscope (Fig. 1).

2.2.1. Microscope setup

The QPM setup, as depicted in Fig. 1(a), is based on Linnik interferometry, consisting of two identical objective lenses (PLN 20X, Olympus, Shinjuku City, Tokyo, Japan) for 20x magnification, or two identical water-immersion objective lenses (LUMPLFL 40X, Olympus, Shinjuku City, Tokyo, Japan) for 40x magnification. For interference image acquisition, light is emitted from a red-light LED (λ = 633 nm) through a Linnik interferometer, that divides the beam into two pathways. Two separated beams are focused with the two identical objective lenses on the sample and the reference mirror. The red-light power on the back aperture of the sample objective lens is 0.32 mW. The beams are then reflected onto the 12-bit CCD camera (acA1920-40um, Basler AG, Ahrensburg, Germany) with the maximum frame rate of 41 fps. The camera data is sent to a PC (Processor core i7, 3.40 GHz) for phase unwrapping analysis. The QPM also has a feedback control system to adjust the Optical Path Difference (OPD) with high resolution, comprised of a laser source (λ = 1.3 μm)(S1FC1310, Thorlabs, Newton, NJ, USA), an infrared Photo-Detector (PD) (62-271, Edmund Optics, Barrington, NJ, USA), a Piezoelectric Transducer (PZT) (AE0505D08F, NEC TOKIN, Shiroishi, Miyagi, Japan), and a DSP-based

Biomedical Optics EXPRESS

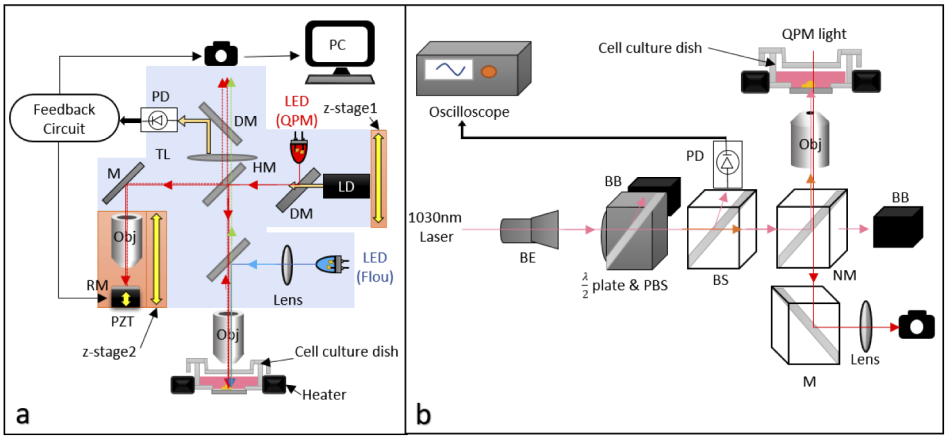

Fig. 1. (a) Quantitative phase and fluorescence microscope setup. PD:Photodiode, LED: light-emitting diode, LD: Laser diode, RM: Reference Mirror, HM: Half Mirror, DM:Dichroic Mirror, M: Mirror, TL: Tube lens, Obj: Objective Lens. To avoid confusion, the reflected beams are colored with strip pattern [33]. (b)Schematic of the LIS setup, BB: BeamBlocker, BS: Beam Splitter, BE: Beam Expander, NM: NIR Mirror, PD: Photodiode, $\frac{\lambda}{2}$ plate: half-wave plate, PBS: Polarized Beam Splitter.

signal demodulation circuit. The PZT on the reference arm can adjust the OPD with a high resolution of <1 nm and a maximum variation of 440 nm, at a frequency of about 500 Hz [31].

For fluorescence microscopy, a blue light LED (λ = 475 nm) is added to the system. To excite the sample, the LED is placed in front of a condensing lens and a mirror with 20% reflectance, to guide the light through the same objective lens that the QPM light passes. The fluorescence light power on the back aperture of the sample objective lens can be up to 4.4 mW. Changing the LED and the mirror is possible based on the desired dye used in the experiment. The emitted light is captured by the camera after passing the objective lens and mirrors.

The system can switch between QPM and fluorescence imaging at a high speed. The software controls the exposure of the LED for the QPM and fluorescence excitation, in short, alternating intervals (every one second) so only one LED is on at a time. The blinking LED also helps to avoid photo-bleaching. Images are processed according to the mode used for image capturing. Cells are cultured on custom-made dielectric mirror bottom dishes (D = 35 mm). The dielectric coating fabricated by Hamamatsu at the bottom of the dish reflects 50% of the visible light. The transmission percentage of the coating at 1030 nm is approximately 92%. The imaging dish is placed in a heating chamber connected to a digital temperature controller (E5CC, OMRON, Kyoto, Kyoto, Japan), to keep the cell medium temperature at 37°C.

2.2.2. LIS setup

A Q-switched diode-pumped solid-state (DPSS) laser (Flare NX, Coherent, Sana Clara, CA, USA) producing pulses of 1.5 ± 0.2 ns at λ = 1030 nm is used to generate LIS. The laser pulses can be generated with a frequency of up to 2000 Hz. To generate laser pulses, the device is connected to a function generator (GFG-8015G, GW Instek, New Taipei City, Taiwan), that can produce a 5 volts square wave with 0.2-2 MHz. The pulses can be generated with a 120 μs delay with each trigger of the function generator.

Laser power is controlled by passing the laser beam through a beam expander and a half-wave plate polarizer. The beam then passes through a polarized beam splitter that directs a portion of it into a photodiode (PDA100A - Si Switchable Amplified Gain Detector, Thorlabs, Newton, NJ, USA) for laser power measurement. The output of the photodiode is connected to a 500 MHz, 2

Biomedical Optics EXPRESS

channel digital oscilloscope (TDS3052B, Tektronix, Beaverton, OR, USA). The rest of the beam is reflected by a NIR mirror and is focused on the cell culture medium from the bottom via a 40x water immersion objective lens (C Achroplan NIR 40x/0.80 W, Zeiss). Also, for measuring the laser power entering the objective lens, a photodiode power sensor (S120, Thorlabs, Newton, NJ, USA) connected to a power and energy meter console (PM400, Thorlabs, Newton, NJ, USA) can be placed in the beam path. For focusing the laser light on the cell medium, another camera (acA1300-30um, Basler AG, Ahrensburg, Germany) is placed under the dish to capture the image of the sample using the same objective that focuses the laser light. The light from the QPM passes through the medium, and since the reflecting mirror is not 100% reflective, a portion of the light passes through the sample and the bottom objective, and is focused with a converging lens, on the second camera. The schematic of the LIS setup can be seen in Fig. 1(b).

Based on the current setup the pulse energy is estimated to be $7.5 * 10^{-5}$ J, the input power is 0.1132 W, and the optical power per unit area at the focus is $2.68 * 10^{8} \frac{W}{m^2}$.

2.3. Cell preparation

Cortical mouse brain tissue was acquired commercially from Brain Bits, LLC (BrainBits animal protocol #32-08-013 was approved by the Southern Illinois University School of Medicine Laboratory Animal Care and Use Committee on 5/18/11). The Brain Bits procedure prior to being shipped to our lab from the company involved dissociation of primary astrocytes from the cortex of E18 mice by an 8-minute incubation with 2 mg/mL papain (Sigma, St. Louis, MO, USA) in Hibernate E (without Calcium and B27, BrainBits, Springfield, IL, USA) medium. Astrocytes were resuspended in a co-culture medium and seeded onto matrigel-coated glass-bottomed dishes. Potorous tridactylis rat kangaroo established epithelial kidney (PTK2) cells stably expressing GFP-gamma tubulin were plated onto 35 mm imaging dishes. Cells were cultured in advanced MEM media as described previously [34]. Cells were in culture in 5% CO2 at 37° for a minimum of 5 days prior to the experiments.

2.4. Image acquisition

The image acquisition was done with a resolution of 1920*1200 and the frame rate of 13.33 fps. As each phase image was constructed from 4 consecutive raw images, the phase image acquisition was done with the frame rate of 3.33 fps and a resolution of 1920*1200. The spatial resolution for the 20x objective lens is 0.30 microns per pixel and for the 40x objective lens is 0.15 microns per pixel.

3. Results

A laser-induced shockwave was applied in the astrocytes medium while the QPM was recording both quantitative phase and phase-contrast (PhC) images of the cells at 40x magnification. The recording started from 20 minutes before LIS to 80 minutes after the application of LIS. The real height of the cells at each time point can be calculated by using the phase values, taken from quantitative phase images, and inserting them in Eq. (2) and (3). To assess the cell injury caused by LIS, the height changes can be measured by taking the difference between the resulting height values before and right after LIS. The phase contrast (PhC) images and the differential interference contrast (DIC) images were obtained computationally, by differentiating the phase map generated by the QPM [35], and subtracting a wavefront shearing operation from the original wave [36], respectively.

Figure 2(a), displays a phase-contrast field of view (FOV) of astrocytes 80 minutes after LIS. LIS has happened on the right side of the FOV, and the red circles shown are concentric with LIS with radii of $75\mu m$ and $150\mu m$. Figure 2(b-e) display the PhC image of the cell in the black rectangle, at different time points with respect to LIS; the negative sign is the time before LIS. The phase-contrast images of the indicated cell before and right after LIS, show no significant

Biomedical Optics EXPRESS

injury. However, the phase-contrast images are not adequate to confirm that the cell has not been affected by LIS, as they cannot quantitatively show height changes. Quantitative phase images of the cell were used to measure the cell height at different time points with respect to LIS. Figure 3 displays the height change measurements for the cell; the purple and green lines show the cell border in former and later time points. Comparing the images from 20 minutes before LIS does not show any flattening or upward movements in the cell (Fig. 3(a)). Comparing the height of the cell just prior and after the LIS suggests no significant changes resulted from the shear stress of LIS (Fig. 3(b)). On the other hand, after 80 minutes, significant morphological changes were detected in this cell (Fig. 3(c)). This figure demonstrates a significant change in the cell morphology in a prolonged time period after LIS. It appears that the cell has flattened morphologically and moved toward the neighboring dying cell. The interactions between these cells may suggest phagocytosis. Phagocytosis response in astrocytes to injured neighboring cells have been also shown in the previous studies [16,37]. 3D video displaying the interactions between this cell and its neighboring cell (Supplement 1, Visualization 1) and a montage of the cell junction at different time points can be seen in supplementary data of the paper.

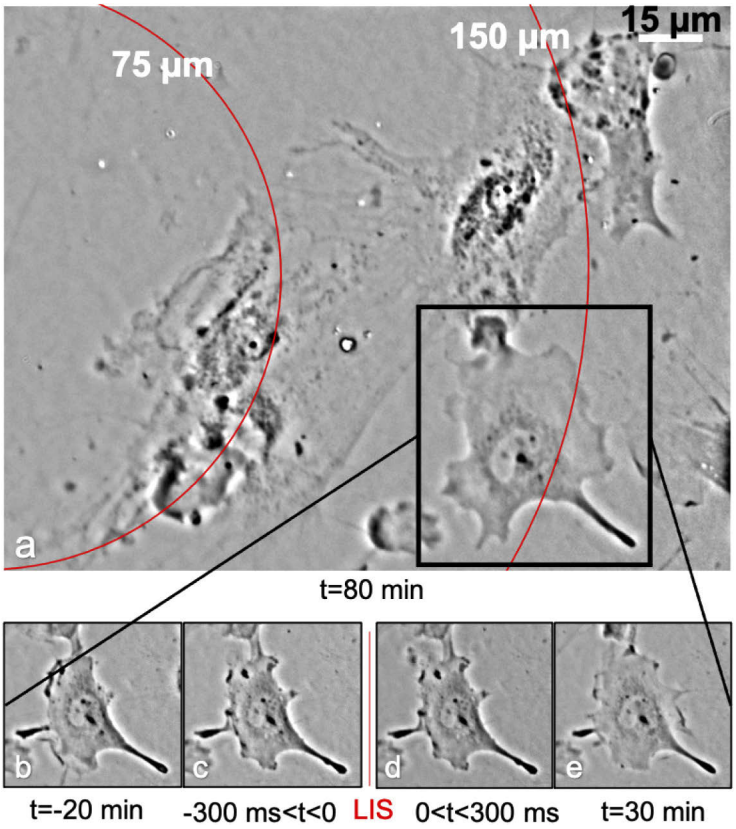

Fig. 2. PhC image of astrocyte cells. **(a)** Whole FOV of cells 80 minutes after LIS. The red circles are care concentric with LIS and have radii of 75 μm and 150 μm. **(b-e)** The PhC image of the cell in the black rectangle, at different time points with respect to LIS. The negative sign means the time before LIS.

To demonstrate the ability of the system to generate repetitive injuries, two consecutive laser-induced shockwaves, with a 1-second interval between LIS exposure, were generated at the same location in the astrocytes medium. Figure 4 illustrates a series of reconstructed 3D

Biomedical Optics EXPRESS

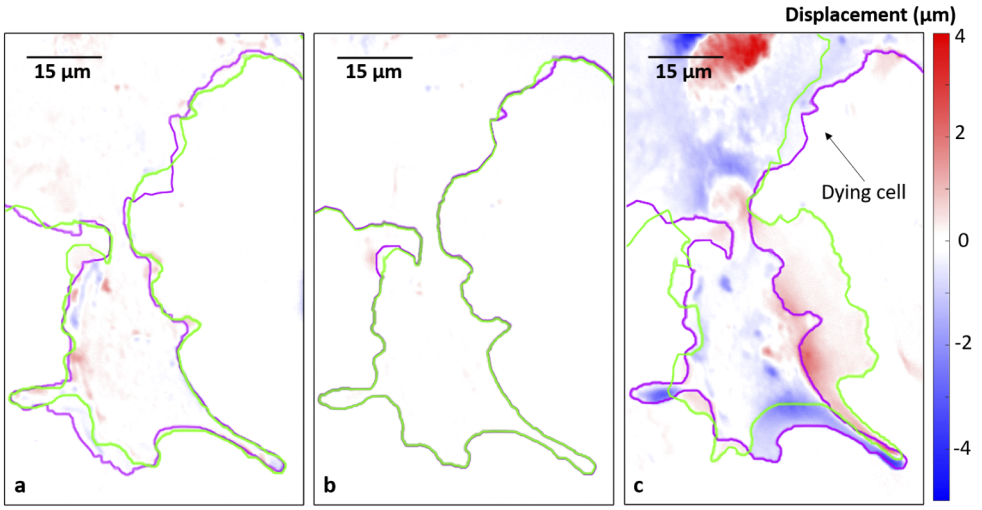

Fig. 3. Height changes in the cell, indicated with a black rectangle in Fig. 2, **(a)** from 20 minutes before to right before LIS, **(b)** from less than 300 ms before LIS to less than 300 ms after LIS, **(c)** from right before to 80 minutes after LIS. All of the figures are calculated by taking the differences of the cell's height at two indicated time points. The purple and green lines show the cell border in former and later time points.

images of the whole FOV encompassing the pre- and post- LIS effects on cells in response to laser-induced shockwaves t_1 is the time of the application of the first LIS and t_2 is for the second LIS). 3D images were made using quantitative phase images, with ImageJ's interactive 3D surface plot plugin. In this series, little or no effects of LIS are detected after the first LIS, but after the second LIS, considerable effects are noticed in the central cell (labelled cell #1), that are magnified in Fig. 4(a,d-f). Figure 4(d) displays the deformation caused by the shear stress right after the second LIS. Moreover, significant changes can be seen in the nucleus and cytoplasm of the cell #2. In this cell, there are distinct changes in the cytoplasm that appear as granulation or fragmentation of cellular components. Though no distinctive internal cellular changes are seen in the QPM images following the first LIS, considerable changes are observed in the nucleus (center) of the cell following the second LIS. A more detailed height change measurement of the cells after the second LIS can be found in the Supplement 1 of the paper.

LIS was also applied to culture medium containing PTK2 cells (Fig. 5). The recording started from 15 minutes before LIS to 45 minutes after the application of LIS. PhC, DIC and QPM images were taken under 20x magnification, while the LIS was applied. Figure 5(a-d) show the PhC and DIC images before and after LIS, respectively. Figure 5(e) displays the quantitative height changes caused by LIS in PTK2 cells. The gradual decrease in the height changes in the cells can be seen as we move further from the center of LIS. It seems that cells indicated with a black rectangle are in the telophase of the mitosis cycle. Although based on the PhC and DIC images, it appears that there is no significant change in the indicated cells, the QPM image shows a significant height change in these cells caused by LIS. Figure 5(f) displays the height profile of the cell along a radial vector, shown with a black line in Fig. 5(e), from the LIS epicenter, before and after the LIS. Using plot profile exact height changes of the cells in the direction of the LIS can be measured.

Biomedical Optics EXPRESS

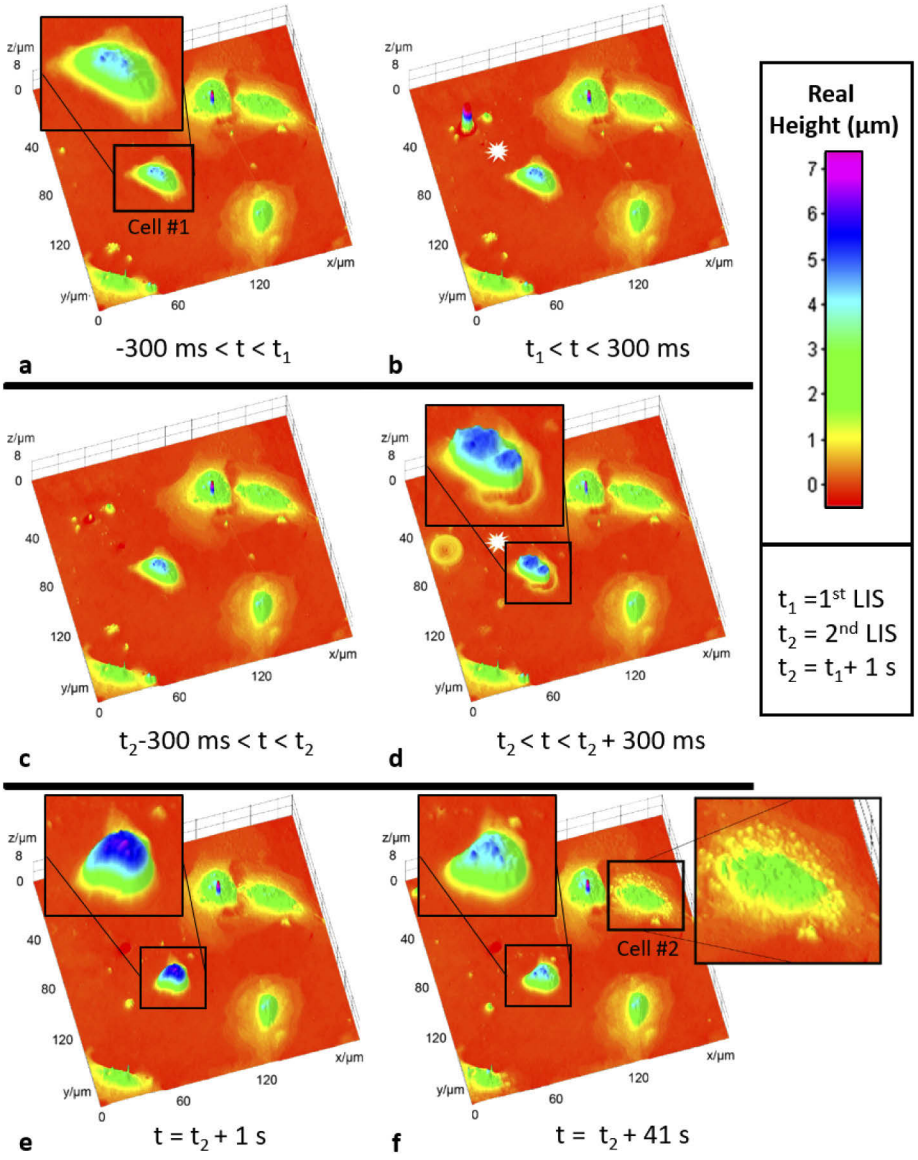

Fig. 4. Reconstructed 3D image of the cells in the field of view. The center of the LIS has been shown with a white star. Cell #1 and cell #2 are magnified in some of the sub-figures. The t indicates the time that each figure has been recorded, that is **(a)** less than 300 ms before the first LIS, **(b)** less than 300 ms after the first LIS, **(c)** 1 s after the first LIS and less than 300ms before the second LIS, **(d)** less than 300 ms after the second LIS (This image shows how cell #1 has been pushed away from the center of the LIS instantaneously.), **(e)** 1 s after the second LIS, **(e)** 41 s after the second LIS. Vacuoles that have been formed in the cell #2 can be clearly seen in this image.

Biomedical Optics EXPRESS

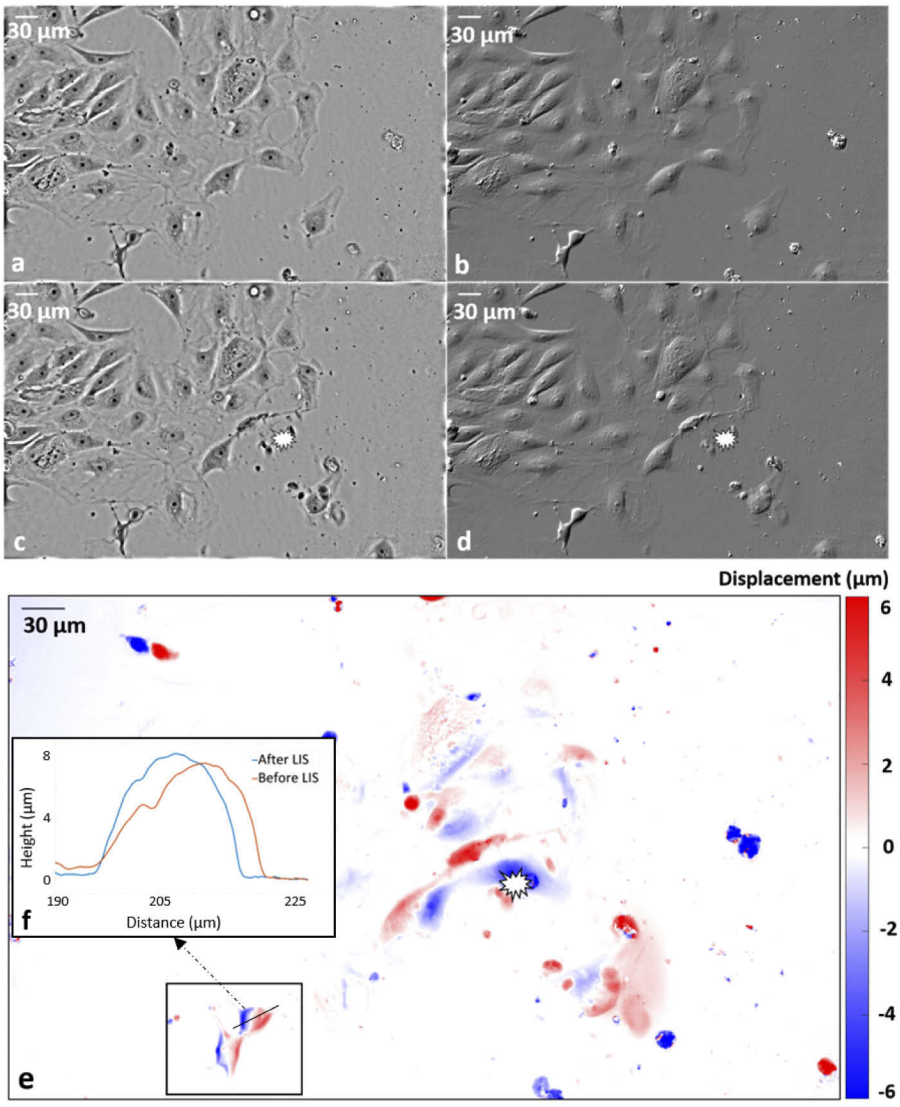

Fig. 5. Images of PTK2 cells with 3 different modalities. The center of the LIS has been shown with a white star. **(a)** PhC image before LIS, **(b)** DIC image before LIS, **(c)** PhC image after LIS, **(d)** DIC image after LIS, **(e)** Quantitative height changes from before to after LIS. Significant height changes from LIS can be seen in the cells indicated with a black rectangle; these height changes cannot be detected in PhC and DIC images. **(f)** The height profile of the cell along a radial vector, shown with a black linee in (e), from the LIS epicenter, before and after the LIS.

Biomedical Optics EXPRESS

4. Discussion

In this paper, we describe a method to observe and study LIS-induced injury to cells. This method is promising for several reasons. Firstly, QPM allows high-resolution imaging of the cells in 3 dimensions. Using real-time phase values, changes in the membrane dynamics, as well as changes in the thickness and structure of the nucleus and cytoplasm, can be measured quantitatively. Secondly, cells can be imaged almost simultaneously with the application of LIS. Cellular changes can be captured immediately after LIS, only limited by the frame rate of the camera. When using methods like LIS, it is crucial to be able to quantify the amount of damage, in order to correlate the cellular responses to the injury. For instance, using QPM, no significant height changes were measured during the application of LIS in the cell indicated in Fig. 2. However, over time, significant changes in the cell's morphology were measured. This suggests that the reaction seen in this cell may probably not be in response to the injury to the cell itself, but it may be in response to its neighboring dying cells; however, more experiments, are needed to confirm this hypothesis. Figure 5 also demonstrates the importance of using QPM while applying LIS. Though no changes were observed in the indicated cells in PhC and DIC images, QPM images revealed a significant amount of change in the cells' thicknesses caused by LIS. As these cells seemed to be in the telophase of the mitosis cycle, this may suggest that the cells in this cycle may be more prone to deformation in response to shear stress. Our future studies will involve more experiments to confirm/reject this hypothesis. Third, cells can be imaged from any period before LIS, continuously to any time after LIS allowing studies on cellular repair over extended periods.

Based on the results presented here, several technical issues can still be improved. Future studies will address the thickness of the mirror placed under the sample dish. The current relatively high thickness of the mirror not only results in laser power attenuation but also damage to the mirror itself, making precise control of laser energy in the focal point difficult. The relatively high mirror thickness also limits the choice of the objective lens that focuses the laser beam. The working distance of these objectives must be greater than 1 mm, thus limiting the optical resolution of the cells and their internal organelles.

The system described here is capable of capturing quantitative phase images, phase-contrast images, and also fluorescence images. The experiments on the fluorescent beads can be found in the Supplement 1 of the paper (S5). With respect to fluorescence images, we should be able to correlate different protein signaling with the changes in the membrane, cytoplasmic, and nucleus dynamics in response to the injury.

5. Conclusion

By integrating QPM with laser-induced shockwaves, we have developed an additional method to study cellular injury. This system allows the application of various degrees of shockwave injury while simultaneously monitoring changes in cell membranes, cell shape, and real-time analysis of intracellular damage and recovery. This system is a promising method to study the role of astrocytes in response to TBI.

Acknowledgments. The authors would like to thank the Hamamatsu company for providing us with the Quantitative Phase Microscope and also their assistance and support. We would like to thank Chung-Ho Sun for her assistance regarding cell culture.

Disclosures. The authors declare no conflicts of interest.

Data availability. Data underlying the results presented in this paper are not publicly available at this time but may be obtained from the authors upon reasonable request.

Supplemental document. See Supplement 1 for supporting content.

Biomedical Optics EXPRESS

References

1. V. Gomez Godinez, S. Kabbara, A. Sherman, T. Wu, S. Cohen, X. Kong, J. L. Maravillas-Montero, Z. Shi, D. Preece, K. Yokomori, and M. W. Berns, "Dna damage induced during mitosis undergoes dna repair synthesis," PLoS One **15**(4), e0227849 (2020).
2. M. W. Berns, "Laser scissors and tweezers to study chromosomes: a review," Frontiers in Bioengineering and Biotechnology **8**, 1 (2020).
3. T. Hunt and R. Westervelt, "Dielectrophoresis tweezers for single cell manipulation," Front. Bioeng. Biotechnol. **8**(3), 227–230 (2006).
4. T. Hayakawa, M. Kikukawa, H. Maruyama, and F. Arai, "Laser-driven gel microtool for single-cell manipulation based on temperature control with a photothermal conversion material," Appl. Phys. Lett. **109**(25), 254102 (2016).
5. Y. Hosokawa, H. Takabayashi, S. Miura, C. Shukunami, Y. Hiraki, and H. Masuhara, "Nondestructive isolation of single cultured animal cells by femtosecond laser-induced shockwave," Appl. Phys. A **79**(4-6), 795–798 (2004).
6. Y. Hosokawa, "Applications of the femtosecond laser-induced impulse to cell research," Jpn. J. Appl. Phys. **58**(11), 110102 (2019).
7. M. O. Steinhauser and M. Schmidt, "Destruction of cancer cells by laser-induced shock waves: recent developments in experimental treatments and multiscale computer simulations," Soft Matter **10**(27), 4778–4788 (2014).
8. A. Sondén, B. Svensson, N. Roman, H. Östmark, B. Brismar, J. Palmblad, and B. T. Kjellström, "Laser-induced shock wave endothelial cell injury," Lasers Surg. Med. **26**(4), 364–375 (2000).
9. C.-P. Yao, Z.-X. Zhang, R. Rahmanzadeh, and G. Huettmann, "Laser-based gene transfection and gene therapy," IEEE Trans. on Nanobioscience **7**(2), 111–119 (2008).
10. A. G. Doukas, "Pressure waves in medicine: From tissue injury to drug delivery," in *AIP Conference Proceedings*, vol. 706 (American Institute of Physics, 2004), pp. 1431–1435.
11. A. Nakagawa, G. T. Manley, A. D. Gean, K. Ohtani, R. Armonda, A. Tsukamoto, H. Yamamoto, K. Takayama, and T. Tominaga, "Mechanisms of primary blast-induced traumatic brain injury: insights from shock-wave research," J. Neurosci. **28**(6), 1101–1119 (2011).
12. S. Tomura, S. Seno, S. Kawauchi, H. Miyazaki, S. Sato, Y. Kobayashi, and D. Saitoh, "A novel mouse model of mild traumatic brain injury using laser-induced shock waves," Neurosci. Lett. **721**, 134827 (2020).
13. V. Gomez Godinez, V. Morar, C. Carmona, Y. Gu, K. Sung, L. Z. Shi, C. Wu, D. Preece, and M. W. Berns, "Laser-induced shockwave (lis) to study neuronal ca2+ responses," Front. Bioeng. Biotechnol. **9**, 97 (2021).
14. C. Carmona, D. C. Preece, V. Gomez-Godinez, L. Z. Shi, and M. W. Berns, "Probing mechanobiology with laser-induced shockwaves," in *Optical Trapping and Optical Micromanipulation XIV*, vol. 10347 (International Society for Optics and Photonics, 2017), p. 103470D.
15. A. Selfridge, D. Preece, V. Gomez, L. Shi, and M. Berns, "A model for traumatic brain injury using laser induced shockwaves," in *Optical Trapping and Optical Micromanipulation XII*, vol. 9548 (International Society for Optics and Photonics, 2015), p. 95480P.
16. N. M. Wakida, G. M. S. Cruz, C. C. Ro, E. G. Moncada, N. Khatibzadeh, L. A. Flanagan, and M. W. Berns, "Phagocytic response of astrocytes to damaged neighboring cells," PLoS One **13**(4), e0196153 (2018).
17. J. E. Burda, A. M. Bernstein, and M. V. Sofroniew, "Astrocyte roles in traumatic brain injury," Exp. Neurol. **275**, 305–315 (2016).
18. F. Zernike, "How i discovered phase contrast," Science **121**(3141), 345–349 (1955).
19. Y. Park, C. Depeursinge, and G. Popescu, "Quantitative phase imaging in biomedicine," Nat. Photonics **12**(10), 578–589 (2018).
20. B. R. Masters, "Quantitative phase imaging of cells and tissues," J. Biomed. Opt. **17**(2), 029901 (2012).
21. N. Pavillon, J. Kühn, C. Moratal, P. Jourdain, C. Depeursinge, P. J. Magistretti, and P. Marquet, "Early cell death detection with digital holographic microscopy," PLoS One **7**(1), e30912 (2012).
22. M. Mugnano, P. Memmolo, L. Miccio, S. Grilli, F. Merola, A. Calabuig, A. Bramanti, E. Mazzon, and P. Ferraro, "In vitro cytotoxicity evaluation of cadmium by label-free holographic microscopy," J. Biophotonics **11**(12), e201800099 (2018).
23. A. Calabuig, M. Mugnano, L. Miccio, S. Grilli, and P. Ferraro, "Investigating fibroblast cells under "safe" and "injurious" blue-light exposure by holographic microscopy," J. Biophotonics **10**(6-7), 919–927 (2017).
24. C. Hu and G. Popescu, "Quantitative phase imaging (qpi) in neuroscience," IEEE J. Sel. Top. Quantum Electron. **25**(1), 1–9 (2019).
25. T. Yamauchi, H. Iwai, and Y. Yamashita, "Label-free imaging of intracellular motility by low-coherent quantitative phase microscopy," Opt. Express **19**(6), 5536–5550 (2011).
26. P. Pouladian, T. Yamauchi, N. M. Wakida, M. W. Berns, and D. Preece, "Simulating traumatic brain injury (tbi) using laser-induced shockwave under quantitative phase microscopy," in *Optical Trapping and Optical Micromanipulation XVII*, (International Society for Optics and Photonics, 2020), 1146321.
27. W. Lauterborn and A. Vogel, "Shock wave emission by laser generated bubbles," in *Bubble dynamics and shock waves*, (Springer, 2013), pp. 67–103.
28. K. R. Rau, P. A. Quinto-Su, A. N. Hellman, and V. Venugopalan, "Pulsed laser microbeam-induced cell lysis: time-resolved imaging and analysis of hydrodynamic effects," Biophys. J. **91**(1), 317–329 (2006).
29. M. Lokhandwalla and B. Sturtevant, "Mechanical haemolysis in shock wave lithotripsy (swl): I. analysis of cell deformation due to swl flow-fields," Phys. Med. Biol. **46**(2), 413–437 (2001).

Biomedical Optics EXPRESS

30. A. Vogel, S. Busch, and U. Parlitz, "Shock wave emission and cavitation bubble generation by picosecond and nanosecond optical breakdown in water," J. Acoust. Soc. Am. **100**(1), 148–165 (1996).
31. T. Yamauchi, H. Iwai, M. Miwa, and Y. Yamashita, "Low-coherent quantitative phase microscope for nanometer-scale measurement of living cells morphology," Opt. Express **16**(16), 12227–12238 (2008).
32. X. Liang, A. Liu, C. Lim, T. Ayi, and P. Yap, "Determining refractive index of single living cell using an integrated microchip," Sens. Actuators, A **133**(2), 349–354 (2007).
33. T. Yamauchi, H. Yamada, K. Goto, H. Matsui, O. Yasuhiko, and Y. Ueda, "Transportable and vibration-free full-field low-coherent quantitative phase microscope," in *Quantitative Phase Imaging IV*, vol. 10503 (International Society for Optics and Photonics, 2018), p. 105031U.
34. N. Wakida, C. S. Lee, E. L. Botvinick, L. Z. Shi, A. S. Dvornikov, and M. W. Berns, "Laser nanosurgery of single microtubules reveals location-dependent depolymerization rates," J. Biomed. Opt. **12**(2), 024022 (2007).
35. M. Mir, B. Bhaduri, R. Wang, R. Zhu, and G. Popescu, "Quantitative phase imaging," Prog. Opt. **57**, 133–217 (2012).
36. L. Miccio, A. Finizio, R. Puglisi, D. Balduzzi, A. Galli, and P. Ferraro, "Dynamic dic by digital holography microscopy for enhancing phase-contrast visualization," Biomed. Opt. Express **2**(2), 331–344 (2011).
37. N. M. Wakida, G. M. S. Cruz, P. Pouladian, M. W. Berns, and D. Preece, "Fluid shear stress enhances the phagocytic response of astrocytes," Front. Bioeng. Biotechnol. **8**, 1290 (2020).